Spatial Variability of Water Temperature within the White River Basin, Mount Rainier National Park, Washington

Andrew S. Gendaszek[1,2], Anya C. Leach[1], and Kristin L. Jaeger[1*]

[1]U.S. Geological Survey, Washington Water Science Center, Tacoma, Washington, 98402, United States
[2]currently at King County Department of Natural Resources and Parks, Seattle, Washington, 98104, United States
*To whom correspondence should be addressed: kjaeger@usgs.gov

This preprint has been superseded by

Gendaszek, A.S., Leach, A.C., and Jaeger, K.L., 2025, Spatial stream network modeling of water temperature within the White River Basin, Mount Rainier National Park, Washington (ver. 1.1, May 2025): U.S. Geological Survey Scientific Investigations Report 2025–5029, 17 p., https://doi.org/10.3133/sir20255029. [Supersedes preprint https://doi.org/10.31223/X5712P.].

Abstract

Water temperature is a primary control on the occurrence and distribution of cold-water species. Rivers draining Mount Rainier in western Washington, including the White River along its northern flank, support several cold-water fish populations, but the spatial distribution of water temperatures, particularly during late-summer base flow between August and September, and the climatic, hydrologic, and physical processes regulating this temperature distribution are not well understood. Spatial stream network (SSN) models, which are generalized linear models that incorporate streamwise spatial autocovariance structures, were fit to mean and seven-day average daily maximum water temperature for August and September for the White River basin located with Mount Rainier National Park. The SSN models were calibrated using water temperature measurements collected between 2010 and 2020. Significant covariates within the best-fit models included the proportion of ice cover and forest cover within the basin, mean August air temperature, the proportion of consolidated geologic units, and snow water equivalent. Statistical models that included spatial autocovariance structures had better predictive performance than those that did not. In addition, models of mean August and September water temperature had better predictive performance than those of seven-day average daily maximum temperature in August and September. Predictions of the spatial distribution of water temperature were similar between August and September with a general warming in the downstream part of main-stem White River compared to cooler water temperatures in the high-elevation headwater streams. Estimated water temperatures for the upper White River model are three to four degrees Celsius warmer for tributaries but one to two degrees cooler for the main stem compared to the regional-scale model. Differences between the upper White River SSN model and the regional-scale SSN model are attributed the upper White River SSN including

water temperature observations specific to the upper White River, whereas water temperature observations from lower elevation streams and downstream of the Mount Rainer National Park boundary were used in the regional-scale model.

Introduction

Changes in the water-temperature and discharge regimes of rivers throughout the western United States have contributed to shifts in the ranges of aquatic species that they support (Reiman and others, 2007; Isaak and others, 2010; Eby and others, 2014). Increasing air temperatures, decreasing winter snowpack and glacial extent, and disturbances from flooding, debris flows, and wildfires have been identified as contributing to past and projected changes in the water-temperature regime of rivers. Ectothermic species such as fish are sensitive to changes in water temperature, which regulates their physiological functions and behavior. Optimal temperatures for some fish like bull trout (*Salvelinus confluentus*) are substantially lower than other salmonids (Selong and others, 2001) with peak growth at rates at average temperatures of 13.2 C and declines in feeding at 16 C resulting in greater reductions in range than less thermally sensitive salmonids like rainbow trout (*Onchorhynchus mykiss*; Isaak and others, 2020), which have peak growth rates at temperature ranges between 17.8 and 24.6 C (Verhille and others, 2016). As a result, bull trout are particularly sensitive to changes in water temperature, especially at the margins of their range where their habitat is easily fragmented by thermal barriers and thermally suitable habitat becomes disconnected. In addition, non-native fish like introduced eastern brook trout (*Salvelinus frontenalis*) may displace bull trout from warmer temperature water due to increased growth rates relative to bull trout (McMahon and others, 2007). As a

result, bull trout may become restricted to headwater streams where cold-water temperatures exist.

The native range of bull trout extends throughout western North America (Haas and McPhail, 2001), including western Washington rivers that drain to Puget Sound. The White River flows from its headwaters on the northeastern flank of Mount Rainier, a glaciated stratovolcano, to its confluence with the Puyallup River before flowing into Puget Sound (fig. 1). Upstream of the confluence with Silver Creek, the upper White River basin drains 159 km^2 and is largely within the Mount Rainier National Park boundary or otherwise part of national forest land. In addition to Endangered Species Act (ESA)-listed bull trout, the upper White River and its tributaries provide spawning, rearing, and migration habitat for non-native, introduced species, including eastern brook trout.

The upper White River and tributaries, including Frying Pan Creek, drain several glaciers (fig. 2), which provide an important component of summer base flow to the White River when direct runoff from precipitation is minimal. In addition, discharge from glacial meltwater buffers downstream water temperature during the summer when water temperatures are near their annual maximum. Additionally, streamflow inputs from groundwater discharge, outflow from cirque lakes, and the melt of seasonal snowpack contribute to base flow and influence the thermal regime of the White River and its tributaries. Limited development has occurred within the upper White River basin; landcover at lower elevations is predominately old-growth evergreen forest and at higher elevations is predominantly bare rock and glacial ice. The maritime climate of the study area is characterized by cool, wet winters, when most of the annual precipitation falls as snow, and warm, dry summers. A strong precipitation gradient occurs from the highest

elevations of the study area on the flanks of Mount Rainier to its lowest elevation point at the confluence of the White River and Silver Creek.

Large, infrequent pulses of coarse sediment from the proglacial headwaters of the White River and its glaciated tributaries are deposited onto the valley floor of the White River (Anderson and Jaeger, 2020). The supply of these coarse sediments exceeds the capacity of the White River to transport these sediments, resulting in a braided morphology of the White River. Migration and avulsions of channels along the White River occur during floods, which typically occur during the late fall and early winter. As a result, flow in the White River during base-flow conditions is distributed across multiple channels that shift location at yearly timescales. The active channel morphology along the upper White River also limits encroachment of riparian vegetation resulting in a wide active channel migration zone that, in places, exceeds 150 meters in width and is several times the wetted channel width of the White River during summer base-flow conditions. In addition, well-sorted, coarse-grained sediment deposited within the White River valley serves as an alluvial aquifer that overlies volcanic bedrock. Smaller tributaries with lower elevation, non-glaciated headwaters, including Shaw, Klickitat, Deadwood, Crystal, and Sunrise Creeks are typically single threaded channels with narrow valley widths, low rates of channel migration, and dense riparian vegetation cover. These smaller tributaries contribute additional discharge to summer base flow that originates from groundwater discharge, snowmelt, and, in some tributaries, outflow from alpine lakes that occupy former glacier cirques.

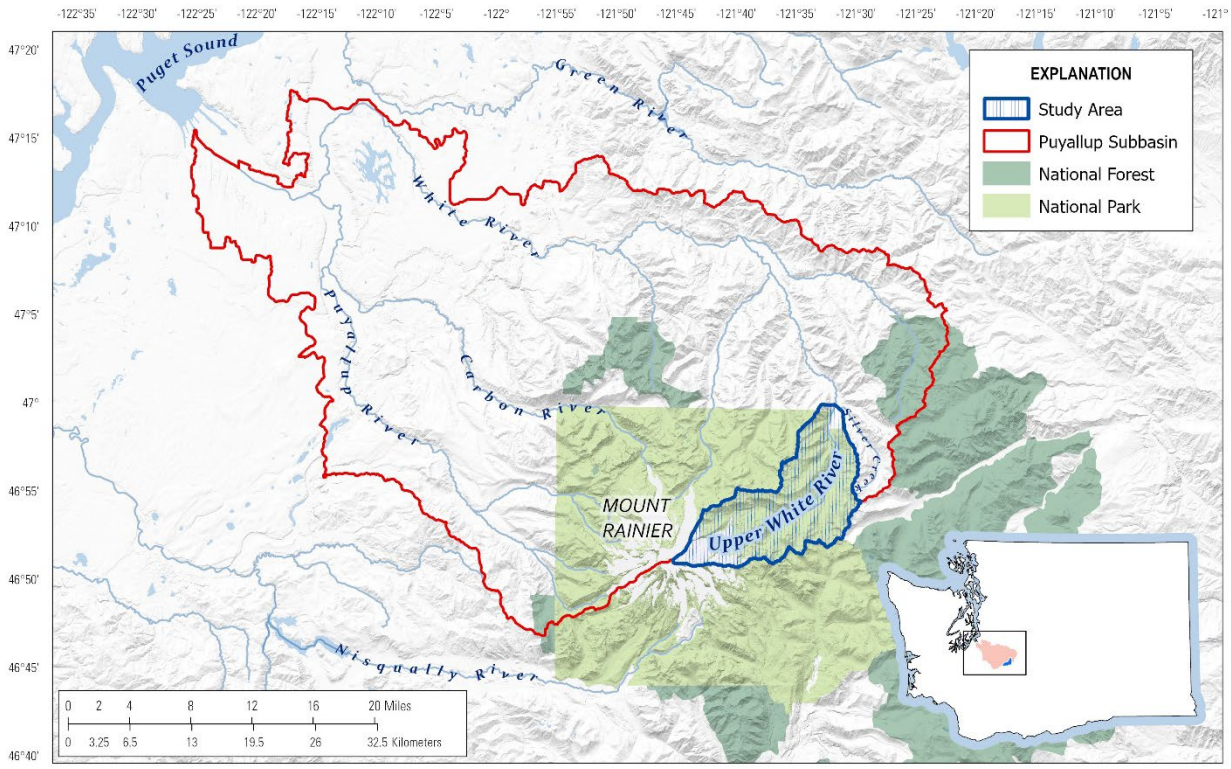

Figure 1. Location of the upper White River basin (study area) within the greater Puyallup River basin and Mount Rainier National Park, Washington.

Spatial variability of water temperature within a river network, termed a thermalscape, is important for natural resource managers to assess the distribution and continuity of habitat for thermally sensitive aquatic species and development of conservation strategies. Statistical models that account for the spatial configuration of the stream network, and which provide spatially continuous estimates of water temperature along a river, can be used to characterize the spatial variability of stream water temperature. These spatial stream network (SSN) models incorporate covariates related to hydrological, meteorological, and other physical processes that influence water temperature. Covariates have been developed at scales ranging from the western United States (NorWeST, Isaak and others, 2017) to individual watersheds (10^3-scale km^2), such as the Snoqualmie River basin in western Washington (Steel and others., 2016) and the Willow

and Whitehorse Creek basin and the Willow, Rock, and Frazer Creek basin in southeastern Oregon and northern Nevada (Gendaszek and others, 2020). Covariates specific to individual basins may account for more local scale factors that influence water temperature but which may not be available in larger regional-scale models, such as the NorWeST model. Mountainous headwater streams with glaciated watersheds, such as the upper White River, have unique factors contributing to water-temperature regimes compared to their lowland counterparts, including glacial meltwater, snowmelt, outflow from alpine lakes, and geologic processes and deposits such as glacial sediment, landslides, and debris flows that contribute to unique groundwater and surface flow conditions within these streams. Therefore, an individual watershed scale modeling approach, which incorporates local covariates and observations specific to the study area, is a promising approach to accurately estimate water temperature in the upper White River basin.

Purpose and Scope

In order to develop a spatially continuous representation of thermal conditions within the upper White River upstream of its confluence with Silver Creek, a spatial stream network (SSN) model was developed using hydrography of the White River basin stream network, measured water temperature, and covariates derived from physical, hydrologic, and climatological processes hypothesized to influence water temperature. The objective of this model was to improve upon regional SSN models (e.g., NorWeST, Isaak and others, 2017) by including spatially intensive water-temperature data collected by the National Park Service and additional covariates specific to the processes influencing water temperature within glaciated headwater streams. The resulting thermalscape will allow natural resource managers to determine the extent and connectivity of thermally suitable habitat for bull trout and other cold-water species within

the White River basin and incorporate information about thermally suitable habitat within habitat conservation plans.

Methods

Water Temperature Data

To support habitat conservation planning for aquatic species within the White River, including bull trout, the National Park Service has maintained a water-temperature monitoring network within the headwaters of the White River basin beginning in 2010 that included data collection at one-hour intervals at 25 sites. Water quality monitoring follows protocols detailed in Rawhouser and others (2012), and data are stored in the publicly accessible National Park Service IRMA database (National Park Service, 2024). Water temperature data measured between 2010 and 2020 were downloaded and summarized based on the site and year those data were collected and are hereafter referred to as site-years. Summary statistics of water temperature relevant to bull trout were calculated that included mean August (AugTw), mean September (SepTw), and seven-day average daily maximum (7DADmax) for August (7DADmaxAug) and September (7DADmaxSep) for each year of the record in order to capture the time of year of maximum water temperatures for this region. Statistics were calculated for 79 site-years that included water-temperature data for at least 90 percent of days within the months of August and September (Figure 2; Table 1). Seventy-three site-years met these criteria for August and September; six site-years met these criteria for the month of September only.

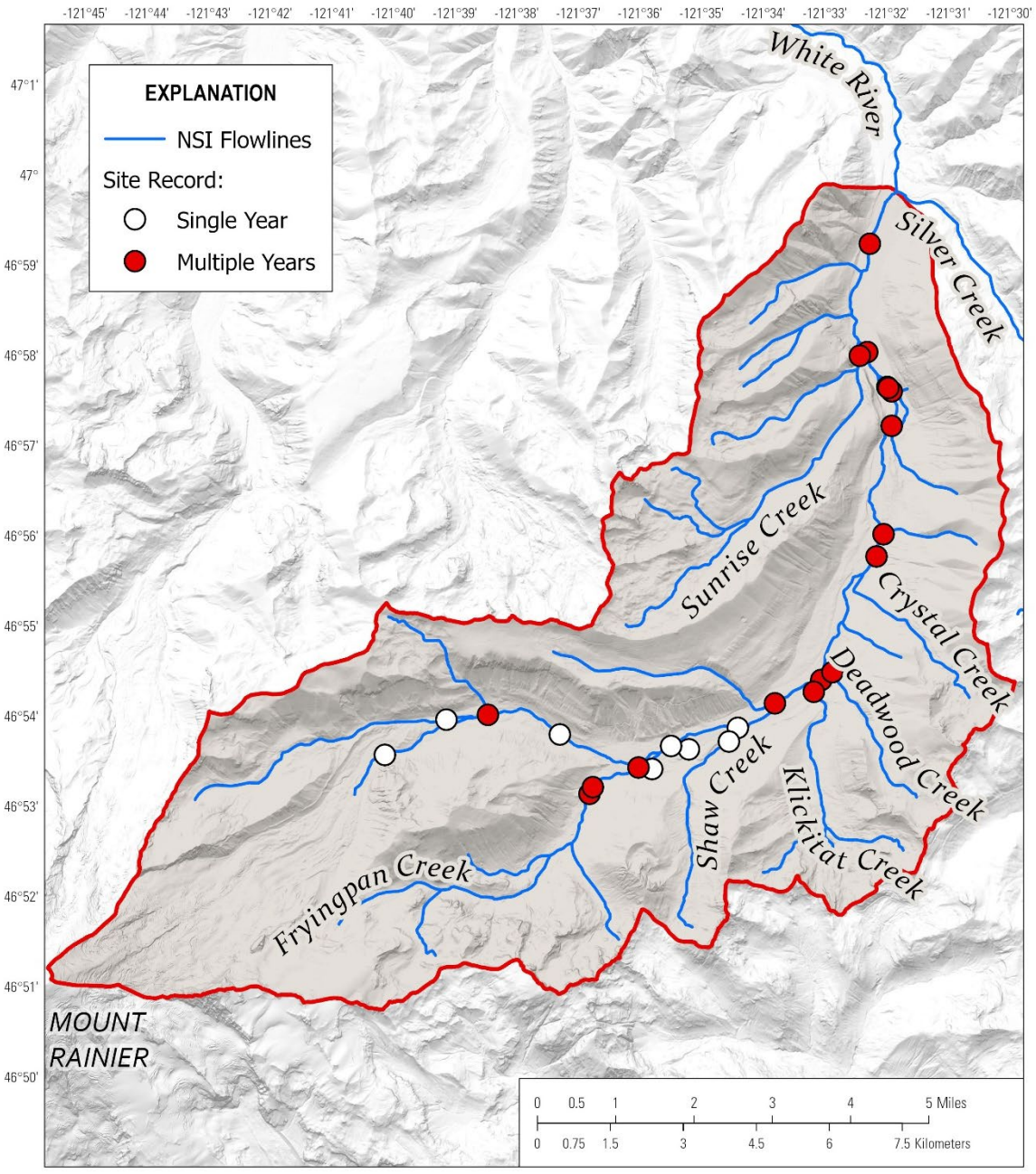

Figure 2. Locations of water-temperature measurement locations along National Stream Intranet (NSI) flowlines included with Spatial Stream Network (SSN) model of water temperature within the upper White River basin, Mount Rainier National Park, Washington.

Table 1. Summary of water-temperature data within the upper White River basin, Mount Rainier National Park, Washington.

Site	Stream	2010	2011	2012	2013	2014	2015	2016	2017	2018	2019	2020
Fryingpan_3820a	Fryingpan Creek	-	-	-	-	-	Aug/Sep	-	Aug/Sep	Aug/Sep	Aug/Sep	Aug/Sep
SG_Frypan	Fryingpan Creek	-	-	-	-	-	-	-	-	-	Aug/Sep	-
w00-00b	White River	-	-	-	-	-	-	-	-	Aug/Sep	Aug/Sep	Sep
w00-00f	White River	-	-	-	-	-	-	Aug/Sep	-	Aug/Sep	Aug/Sep	Aug/Sep
w00-00g	White River	Aug/Sep	Aug/Sep	-	-	Aug/Sep	Aug/Sep	-	-	-	-	-
w00-00h	White River	-	Aug/Sep	Aug/Sep	Aug/Sep	-	Aug/Sep	-	-	Aug/Sep	-	Aug/Sep
w00-00l	White River	-	-	-	-	-	-	-	-	Aug/Sep	Aug/Sep	Aug/Sep
w00-00n	White River	-	-	-	-	-	-	-	-	Aug/Sep	-	-
w00-00n_b	Unnamed Tributary	-	-	-	-	-	-	-	-	-	Aug/Sep	-
w00-00o_n	White River	-	-	-	-	-	-	-	-	-	-	Aug/Sep
w00-00s	White River	-	-	-	-	-	-	-	-	-	-	Aug/Sep
w00-10.5a	White River	-	-	-	-	-	-	-	-	Aug/Sep	-	Aug/Sep
w00-15a	Shaw Creek	-	-	-	-	-	-	-	-	-	-	Aug/Sep
w06-00a	White River	-	-	-	-	-	-	-	-	Aug/Sep	Aug/Sep	Aug/Sep
w07-00a	White River	-	Aug/Sep	Aug/Sep	Aug/Sep	Aug/Sep	Sep	Aug/Sep	Aug/Sep	Aug/Sep	Aug/Sep	Aug/Sep
w09-00a	Unnamed Tributary	-	-	-	-	-	-	-	-	-	Aug/Sep	Aug/Sep
w12-00a	Deadwood Creek	-	-	-	-	-	-	-	-	Aug/Sep	-	Aug/Sep

w13-00a	Klickitat Creek	Aug/Sep	-	Aug/Sep	Aug/Sep	Aug/Sep	Sep	Aug/Sep	Aug/Sep	Aug/Sep	Aug/Sep	Aug/Sep
w14-00a	Unnamed Tributary	-	-	-	-	-	-	-	-	Aug/Sep	-	Aug/Sep
w16-00a	Unnamed Tributary	-	-	-	-	-	-	-	-	-	-	Sep
w17-00a	Fryingpan Creek	-	-	-	-	-	Aug/Sep	-	Aug/Sep	Aug/Sep	-	-
w19-00a	White River	-	-	-	-	Aug/Sep	Aug/Sep	-	Aug/Sep	Aug/Sep	-	Aug/Sep
w21-00b	Inter Fork of the White River	-	-	-	-	-	-	-	-	-	-	Aug/Sep
White_2830a	White River	-	-	-	Sep	Aug/Sep	Aug/Sep	-	Aug/Sep	Sep	Aug/Sep	-
SG_White	White River	-	-	-	-	-	-	-	-	-	Aug/Sep	-

Statistical Models of Stream Temperature

Statistical models of stream temperature were developed using SSN models, which are a class of generalized linear models that account for spatial autocovariance within a stream network (Ver Hoef and Peterson, 2010). SSN models that use a Gaussian distribution have been applied to provide continuous, spatially distributed predictions throughout a stream network, including the distribution of species, water-chemistry data, and water temperature. Many SSN modeling efforts have focused on predicting the spatial distribution of water temperature because of water temperature's fundamental role in determining the occurrence, distribution, and abundance of ectothermic species. SSN models have been developed at broad geographical extents that include the western United States and which include future conditions under projected climate scenarios (NorWeST; Isaak and others, 2017). SSN models have also been developed for individual watersheds in the Pacific Northwest and Great Basin of the United States to inform the availability and connectivity of habitat for cold-water salmonids, including Chinook salmon (*Oncorhynchus tshawytscha*) and Lahontan Cutthroat Trout (*Oncorhynchus clarkii henshawi)* (Steel and others, 2016; Gendaszek and others, 2020). The value of individual watershed scale models is that they generally include new calibration data not included in the larger regional model and also can make use of co-variates specific to the individual watershed that may be effective predictors of water temperature that capture local processes but are not available for use at larger geographic extents and therefore not able to be used in the regional model.

Spatial Stream Network Model Development

SSN models of the upper White River basin were developed from National Stream Intranet (NSI) hydrography processed from the medium-resolution National Hydrologic Dataset version 2 (NHDv2) for topological consistency. Hydrographic features, including braided channels, complex confluences with more than two tributaries, and divergent channels, were removed within the NSI hydrography. The locations of water-temperature measurement sites were moved to coincide with the NSI hydrography and water-temperature prediction sites were created every 100 meters along the NSI hydrography. Spatial and topological attributes were assigned to temperature measurement and prediction sites based on their topological relation to each other using Spatial Tools for the Analysis of River Systems (STARS; Peterson and Ver Hoef, 2014).

Forty covariates representing physiographic conditions and climatic characteristics developed by Jaeger and others (2023a) to model streamflow permanence within Mount Rainier National Park, including the headwaters of the White River basin study area, were considered for inclusion within the SSN models of water temperature within the headwaters of the White River basin. Physiographic characteristics described geology, terrain, soils, and landcover of Mount Rainier National Park; climatic characteristics described precipitation, air temperature, evapotranspiration, and snowpack of Mount Rainier National Park. Jaeger and others (2023a) presented these covariates within flow-conditioned parameter grids (FCPGs; Jaeger and others, 2023b) that allowed continuous representation of covariates across the Mount Rainier National Park study area by providing basin average values that incrementally change as drainage area accumulates in the downstream direction. Parameter grids are 30-m resolution and correspond to the NHDv2 hydrography.

Although water temperature and streamflow permanence are distinct properties of a hydrographic network, the hydrological and climatological processes that influence these properties are often inter-related. In alpine headwater streams, for example, the presence and extent of a seasonal snowpack or glacial ice not only contributes to snowmelt and glacial meltwater runoff that support streamflow but also cools water temperature. Groundwater discharge supports streamflow and imparts a distinct temperature signal on surface water identified as cooling surface water during the summer and warming it during the winter. Of the 40 covariates incorporated within the streamflow permanence model (Jaeger and others, 2023a), the five most important covariates in predicting streamflow permanence (upstream drainage area, total curvature, proportion of consolidated geologic material, topographic wetness index, and proportion forested land cover) were incorporated into the water-temperature SSN model (Table 1; Figure 3). In addition to these five most important covariates for the streamflow permanence model, three additional covariates were incorporated into the water-temperature SSN model to account for the influences of air temperature, glacial ice melt, and seasonal snowmelt on water temperature: cumulative proportion ice cover, March to September snow water equivalent (SWE), and mean daily maximum air temperature (March to September) (Leach and others, 2024). Cumulative proportion ice cover is included in Jaeger and others (2023a). March to September SWE for years between 2010 and 2020 are not included in Jaeger and others (2023a) and were not processed as FCPGs. Instead, SWE values from the unprocessed grids were used. Covariate dataset sources are provided in Table 2.

Table 2. Descriptions of covariates included in spatial stream network (SSN) models of August and September mean water temperature (AugTw, SeptTw, respectively). Parenthetical signs within cells describing hypothesized influences indicate positive (+) or negative (−) relationships with water temperature or flow presence. Details on sources are provided in the text.

Class	Covariate	Abbreviation	Resolution (m)	Scale	Hypothesis	Source
Terrain	Upstream drainage area	Upstream_DA	30	Area weighted	(-) Larger upstream drainage area corresponds to 1) wider streams are proportionally less shaded and 2) lower elevation which have warmer air temperatures	Horizon Systems Corporation (2013)
Terrain	Total curvature	Curve	30	Area weighted	(+) Higher curvature should correspond to increased convergence of streamflow and input of groundwater	Horizon Systems Corporation (2013)
Terrain	Topographic wetness index	TWI	30	Area weighted	(+) The TWI integrates input of water from upslope to drainage of water downslope. A higher TWI corresponds to increased likelihood of water presence and thus cooler temperatures	Horizon Systems Corporation (2013)
Geology	Proportion of basin consolidated geologic material	Geo_Consolidated	12	Area weighted	(+) Higher curvature should correspond to increased convergence groundwater, which is generally cooler than surface water during the summer, and potential for its discharge into the stream	WADNR (2016)
Landcover	Proportion of basin forested land cover	LC_Forest	30	Area weighted	(+) A higher proportion of forested land cover corresponds to increased riparian shading of stream resulting in cooler water temperatures.	Homer and others (2015)

Landcover	Proportion of basin ice landcover	LC_Ice	30	Area weighted	(+) A higher proportion of ice land cover corresponds to increased glacial ice runoff resulting in cooler stream temperatures.	Homer and others (2015)
Climate	Snow Water Equivalent (March - September)	SWE	1000	Local	(+) A higher proportion SWE corresponds to increased potential for snowmelt runoff resulting in cooler stream temperatures.	Barrett (2013)
Climate	Average daily maximum temperature (August and September)	Aug_Ta, Sep_Ta	4000	Area weighted	(-/+) Higher air temperatures may warm stream through conduction associated solar radiative inputs during clear days with higher insolation, but also contribute higher rates of runoff from basins with glacial ice melt and snow melt that contribute to cooler stream temperatures.	PRISM Climate Group (2021)

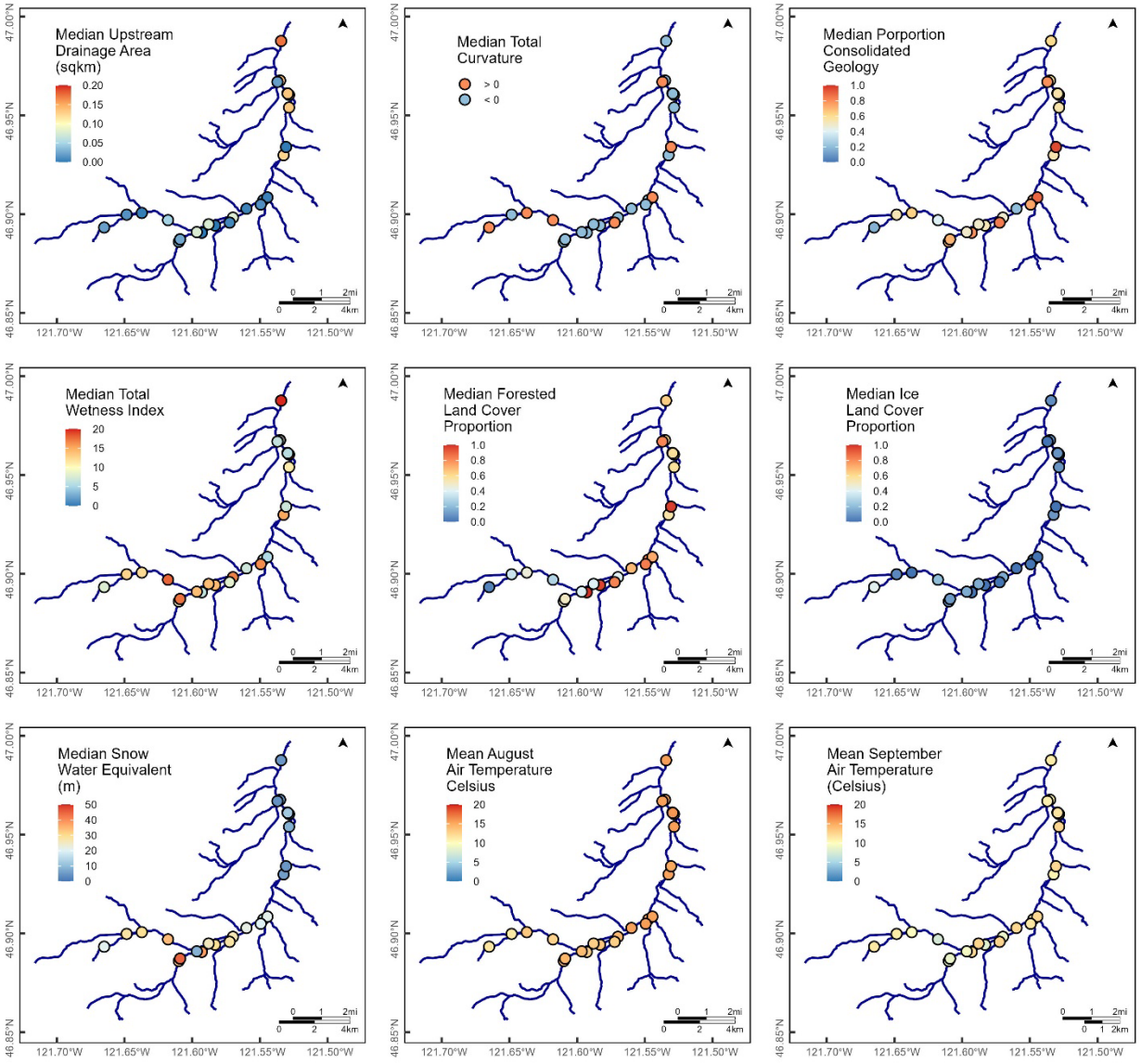

Figure 3. Spatial distribution of covariates included within Spatial Stream Network Model of the upper White River basin: median upstream drainage area, median total curvature, median proportion of consolidated geologic material, median topographic wetness index, median proportion forested land cover, median proportion snow/ice land cover, median snow water equivalent, mean August air temperature, and mean September air temperature. Air temperature covariates are presented as averages of years of water-temperature measurements for each location.

Four sets of models were developed to predict response variables of two metrics of water-temperature magnitude, mean monthly temperature and maximum monthly 7-DADMax, for both the months of August and September, for a total of four response variables. The 7-DADMax is a standard water quality metric typically used to describe relatively short-term conditions compared to monthly averages at a timescale that is relevant to aquatic organisms and is a standard metric in Washington State water quality criteria. Each set of models included 1) a spatial model with autocorrelation structures that included a mixture of exponential tail-up, exponential tail-down, and Euclidean and 2) a non-spatial model that excluded these spatial autocorrelation functions (Ver Hoef and Peterson, 2010). The non-spatial model is included here for comparison against the spatial model in order to evaluate if adding the spatial component to the model improves model fits and results in more accurate estimates of water temperature. The models were fit to the four response variables AugTw, SepTw, August 7-DADMax, and Sep 7-DADMax. Random effects for year were included within each of the spatial and non-spatial models for the four response variables to account for variability across multiple years. Model performance was assessed by calculating mean absolute prediction error (MAPE) between observed temperatures and leave-one-out cross-validation (LOOCV) predictions, root mean square prediction error (RMSPE) from LOOCV prediction, and predictive r^2 calculated as the square of the correlation coefficient between observed temperatures and LOOCV predictions. For each of the four models, non-significant covariates were sequentially removed by applying the equivalent of a backward stepwise regression (Detenbeck and others, 2016). Details of the SSN model, including co-variate values and modeling steps, are presented in Leach and others (2024). Results of the final model were compared to modeled water temperature values from NorWeST.

Results

Spatial stream network models that included spatial autocorrelation structures predicted all four modeled response variables, AugTw, SepTw, August 7-DADMax, and Sep 7-DADMax, better than non-spatial models that excluded spatial autocorrelation structures (Table 3). The highest performing model, the spatial model of AugTw, for example had a predictive r^2 of 0.76 whereas its non-spatial counterpart had a predictive r^2 of 0.23; correspondingly, MAPE and RMPSE increased from the spatial to the non-spatial models indicating decreased model performance. Both spatial and non-spatial model performance metrics were higher for models of mean monthly water temperature compared to monthly 7-DADMax and were higher for models of metrics of August water temperature compared to metrics of September water temperature.

Table 3. Model fit of Spatial Stream Network (SSN) models of water temperature within the upper White River basin, Mount Rainier National Park, Washington. Covariate significance (p-value): 0.1 (.), 0.05 (*), 0.01 (**), and 0.001 (***).

	Response Variable			
	AugTw	7-DADMax Aug Max	SepTw	7-DADMax Sep Max
Sample Size	71	71	77	77
	Spatial Models			
y-intercept	8.74 ***	8.67 ***	5.32 ***	7.75 **
	Covariate coefficient (significance)			
Mean August Air Temperature	-	0.24 ***	-	-
Mean September Air Temperature	-	-	-	-
Upstream Drainage Area	-	-	-	-
Total Curvature	-	-	-	-
Consolidated Geology	-	-2.90 ***	-	-
Total Wetness Index_Local	-	-	-	-
Proportion Forested Land Cover	-	-	3.74 *	-
Proportion Ice Land Cover	-12.54 ***	-	-5.88 .	-
Snow Water Equivalent	-	-0.0003 ***	-	-
	Model Performance			
predicted r^2	0.76	0.67	0.62	0.20
RMSPE	0.74	1.36	0.81	2.26
MAPE	0.49	0.64	0.51	1.23
	Non-Spatial Models			
y-intercept	3.57 *	6.50 ***	5.8 ***	6.10 ***
	Covariate coefficient (significance)			
Mean August Air Temperature	3.82 ***	-	-	-
Mean September Air Temperature	-	-	-	-
Upstream Drainage Area	-	0.00002 ***	0.00001 ***	0.00002 ***
Total Curvature	-	-	-	-
Consolidated Geology	2.78 *	4.83 *	2.48 *	4.60 *
Total Wetness Index_Local	0.08 **	-	-	-
Proportion Forested Land Cover	-3.23 **	-	-	-
Proportion Ice Land Cover	-11.5 ***	-	-10.0 ***	-
Snow Water Equivalent	-	-	-	-
	Model Performance			
predicted r^2	0.22	0.12	0.32	0.08
RMSPE	1.30	2.22	1.07	2.14
MAPE	1.05	1.88	0.77	1.75

Covariates that were significant varied among the four individual response variable models for both the spatial and non-spatial models. Within the spatial models, the proportion of basin ice cover (LC_Ice) was highly significant for the mean August temperature model (AugTw, significance at 0.001), whereas proportion of basin forest land cover was significant (significance at 0.05) for the mean September temperature model (SepTw) in addition to LC_Ice (significance at 0.1). Mean August air temperature (AugTa), proportion of basin consolidated geology (Geo_Consol), and snow water equivalent (SWE) were significant covariates for the 7-DADMaxAugMax model; no significant covariates were identified in the 7-DADMaxSepMax model. Topographic variables of drainage area (UpFAC), curvature (Curve) and total wetness index (TWI) were not significant variables in any of the spatial models. For the non-spatial models, upstream flow accumulation area (UpFAC) and proportion of basin consolidated geology (Geo_Consol) were consistent significant covariates in three out of four and all four response variable models, respectively (Table 3).

The spatial distribution of predicted AugTw, SepTw, August 7-DADMax, and September 7-DADMax for the final model varied within the upper White River basin primarily with respect to longitudinal position within the drainage network and connection to or disconnection from glacial meltwater, as represented by proportion of ice (figs. 3 and 4). In general, water temperatures as characterized by all four response variables increased downstream from high-elevation headwater streams to the downstream extent of the model domain at the White River-Silver Creek confluence. The coolest tributaries to the main-stem White River received direct contributions of glacial meltwater whereas tributary streams that did not receive glacial meltwater were warmest as measured by each of the four response variables.

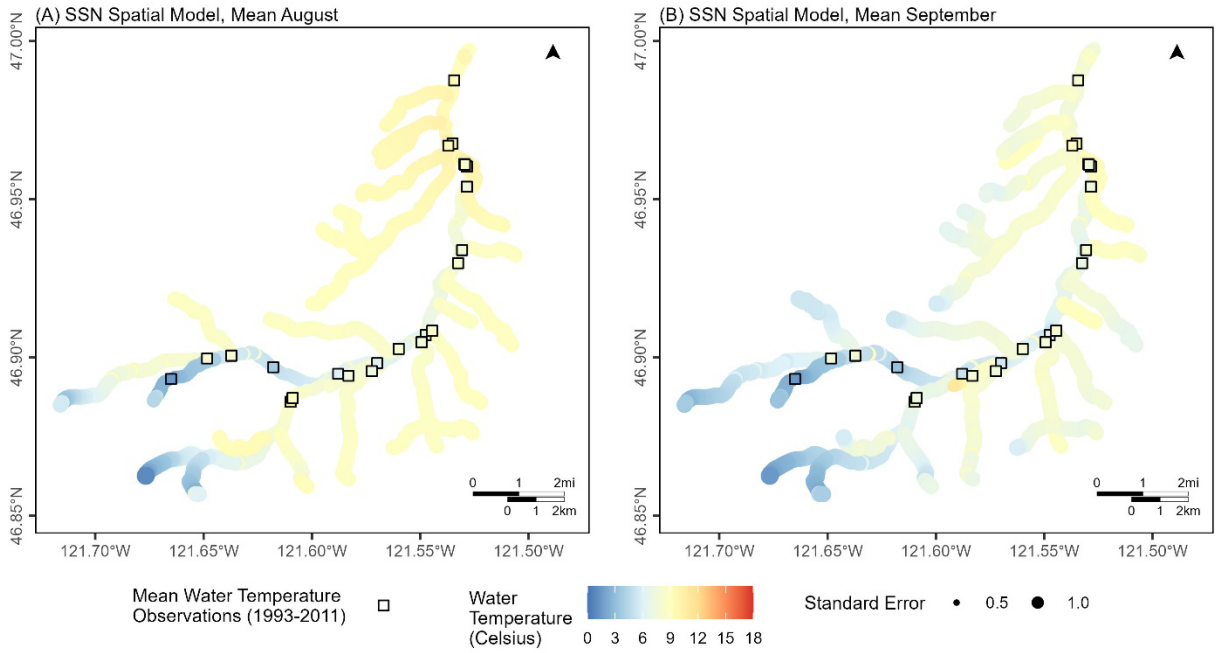

Figure 4. Predicted values of mean August water temperature (AugTw) and September water temperature (SepTw) by Spatial Stream Network models that included the spatial autocovariance structure.

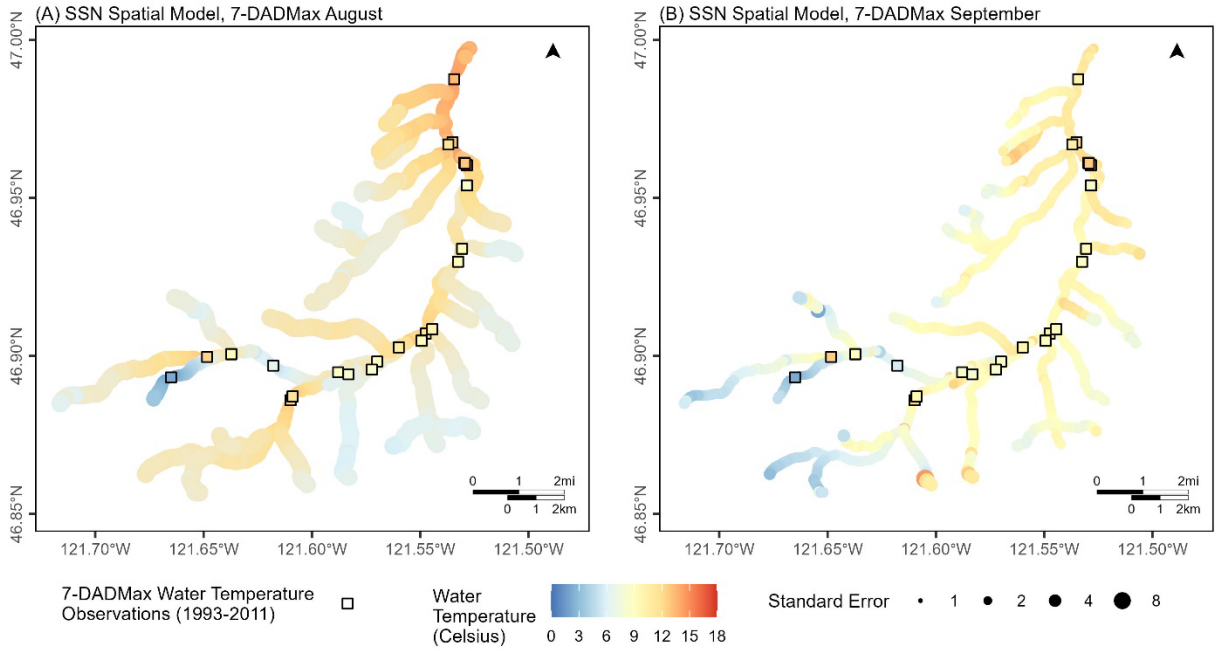

Figure 5. Predicted values of August and September 7-Day Average Daily Maximum (7-DADMax) water temperature by Spatial Stream Network models, including the spatial autocovariance structure.

On average, mean average August temperature is approximately one degree Celsius warmer in the upper White River SSN model compared to the modeled temperature from the NorWeST SSN model (Table 4). Warmer overall temperature for the study area is attributed to warmer temperatures by three to four degrees Celsius in tributaries draining to the main stem in the upper White River SSN model compared to the NorWeST SSN model (Figure 6). However, the upper White SSN model has cooler temperatures by approximately three degrees Celsius in reaches immediately draining glaciers and cooler temperatures in the main stem by approximately one to two degrees Celsius (Figure 6). Water temperature observations used to calibrate the NorWeST model were located in lower elevation river reaches farther from the glacierized regions of Mount Rainier whereas the upper White River SSN model was calibrated using observations from the upper White River main stem, including reaches in close proximity to the glaciers and in non-glacierized tributaries (Figure 2, Table 1).

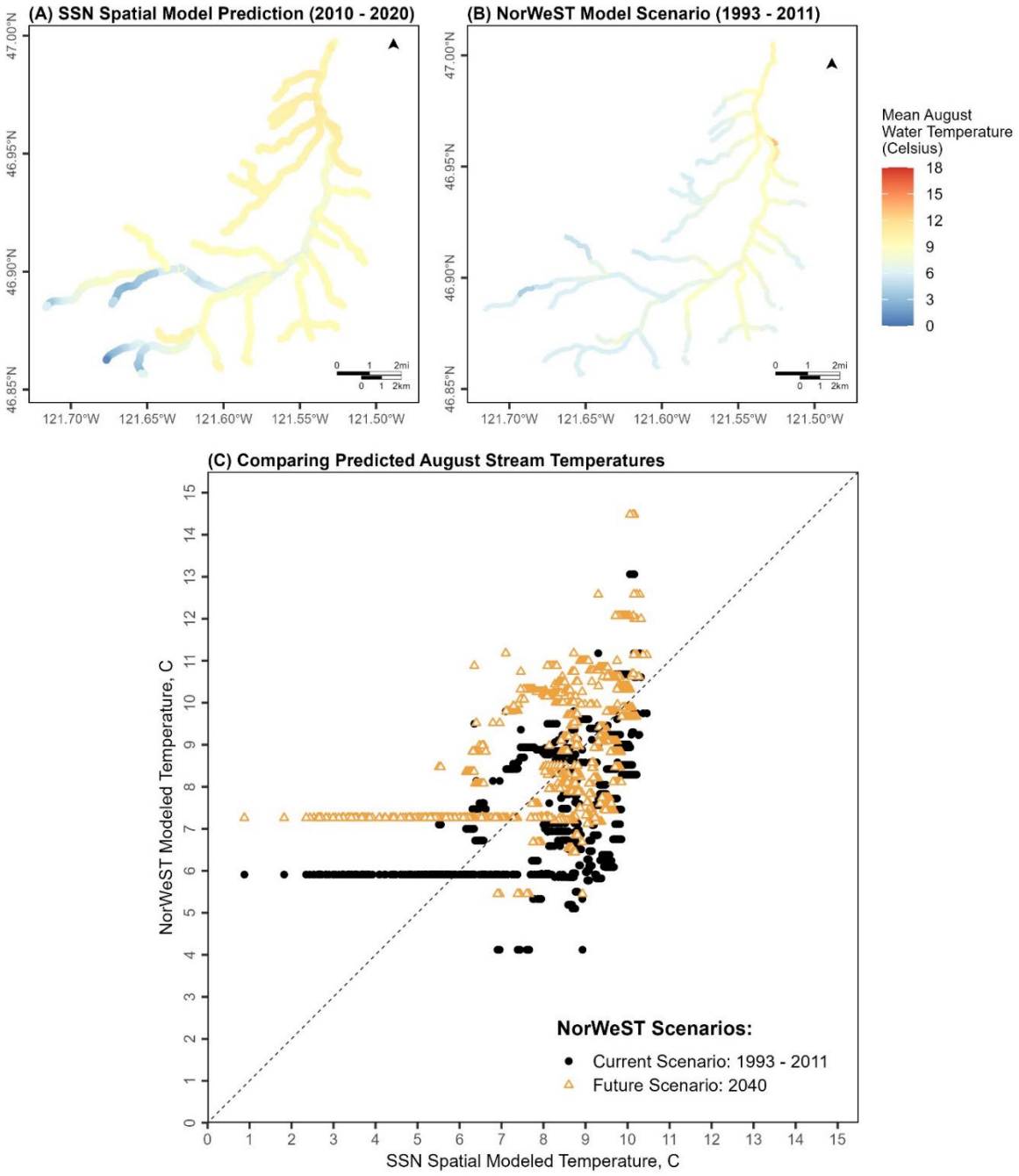

Figure 6. Predicted values of mean August water temperature by Spatial Stream Network (SSN) models, including the spatial autocovariance structure for 2010 to 2020 (A) as well as by the NorWeST model Scenarios (Isaak and others, 2017) for 1993 to 2011 (B). The SSN spatial model values are compared to the NorWeST model scenarios for 'current' conditions (1993 – 2011) and future scenario based on global climate model ensemble averages for 2040 (C).

Table 4. Summary of upper White River Spatial Stream Network (SSN) model and the NorWeST water temperature model in degrees Celsius.

		Min	Mean	Max
SSN Spatial Model Predictions	Mean August water temperature from 2010 to 2020	0.9	8.2	10.5
	Scenario of mean August stream temperature from 1993 to 2011	4.1	7.3	13.1
	Future scenario based on global climate model ensemble averages for 2040	5.5	8.6	14.5
NorWeST Model Scenarios	Future scenario based on global climate model ensemble averages for 2080	6.4	9.6	15.4

Discussion

Spatial variability of late-summer water temperature within the White River basin of Mount Rainier National Park was estimated by fitting SSN models that incorporated covariates representing hydrologic, climatic, and physical processes hypothesized to drive the water temperature of the White River and its tributaries. The temperature metrics, AugTw, SepTw, 7DADmaxAug, and 7DADmaxSep, represented the magnitude of water temperature during late-summer base flow when water temperature was near its annual maximum and discharge was near its annual minimum were correlated. However, different covariates representing various drivers of the White River basin's thermal regime were significant and the performance of models fit to each response variable varied such that models of AugTw and SepTw had better predictive performance, than models of 7DADmaxAug and 7DADmaxSep, which we attribute to the relatively coarse resolution of the predictor variables to the response variables resulting in better predictions of average conditions over longer time periods (e.g., monthly versus seven days). Specifically, the monthly models had lower RMSPE and MAPE despite slightly lower predicted r^2 in the SepTw relative to 7DADMax Aug (Table 3). The inclusion of spatial structures, similar

to other statistical models of water temperature within a stream network (e.g., Isaak and others, 2017) substantially improved predictive performance and therefore the spatial models are the final selected model to estimate water temperature compared to the non-spatial model. The relative importance of the hydrologic, climatic, and physical processes hypothesized to drive the White River's thermal regime was evaluated based on covariate significance covariates within best-fit stream temperature models.

During August, when precipitation was at its annual minimum and air temperature was near its annual maximum, surface-water runoff from rainfall and snowmelt was minimal within the White River basin and streamflow was largely maintained by glacial meltwater within streams draining glaciated headwaters. Streamflow within streams draining non-glaciated headwaters of the White River basin, which were generally at lower elevations, is likely largely sustained during August by either groundwater discharge or surface-water outflow from lakes occupying headwater cirques formed by former glaciers that melted during the Holocene. Consequently, August water temperatures within the White River basin differed between those parts of the stream network with glacierized (e.g., covered by glaciers) and non-glacierized headwaters with the colder water temperatures associated with streams immediately draining glaciers (fig 4A and 5B). The best-fit SSN model of AugTw predicted the coldest water temperatures within streams draining the glacierized parts of the upper White River basin with increases in water temperature in the downstream direction attributed to both cumulative radiative inputs from insolation and the input of non-glaciated tributaries downstream. Although the main-stem White River retained cold water temperatures downstream, water temperature predicted by the best-fit SSN model of AugTw gradually increased downstream reflecting both warming due to effect of. Of the covariates considered for inclusion within the AugTw model,

the proportion of basin ice landcover (LC_Ice) was the only significant covariate within the best-fit SSN model that included spatial autocovariance structures. This suggested that hydrological processes connected to the extent of glacial ice were the dominant drivers of stream temperature within the White River basin and best explained the variability of AugTw at measured.

Although the only significant covariate within the best-fit SSN model of AugTw was the proportion of basin ice landcover, other processes likely contribute to the temperature regime of non-glacierized watersheds. However, the limited number of observations within non-glacierized parts of the stream network likely reduced their influence within the best-fit model of AugTw. Consequently, relatively high AugTw within the non-glaciated parts of the White River basin was simply reflected in the model as an absence of glacial ice. Nevertheless, other factors, such as the quantity of groundwater discharge as related to subsurface geology and riparian shading as reflected through forest cover, likely contributed to the temperature regime of unglaciated basins despite their overall influence within the White River being much less than the extent of glacial ice cover. Although performance metrics were slightly lower compared to the two monthly models, SWE was identified as a significant predictor for the 7DADMax Aug model (Table 3). Years of larger snowpack have correlated to cooler water temperatures in other regional mountain rivers (Jaeger and others, 2017). The presence of SWE as a significant predictor in the 7DADMax Aug suggests that larger snowpack years may result in reducing maximum temperatures at least in August, but did not significantly influence average monthly temperatures, at least with this dataset, indicating that the magnitude of snowpack years for this dataset was not sufficient to result in a statistically significant effect on temperature when averaged over a longer time step of one month compared to seven days.

Mean water temperatures in September (SepTw) within the White River basin were lower than mean water temperatures within August (AugTw), but their spatial distributions throughout the White River and its tributaries within each month were similar. The lowest water temperatures, both observed and modeled, were present within those parts of the drainage network receiving glacial meltwater runoff, whereas those parts that did not receive glacial meltwater were warmer (figs 4 and 5) The proportion of basin ice landcover was also a significant covariate within the model of mean September water temperature, but its significance was less relative to the model of mean August water temperature. Diminished significance may be because August temperatures are generally higher than September temperatures and therefore any influence on temperature may be lower for months in which seasonal cooling processes, such as seasonal changes in air temperature, may be more influential. An additional covariate, proportion of basin forested landcover, emerged as a significant covariate within the mean September water temperature model, but its positive relation to SepTw was opposite the hypothesized negative relation, which was based on the assumption that increased forest cover corresponded to increased riparian shading. Although riparian shading was likely higher within parts of the drainage network with a greater proportion of forest landcover, this relation was confounded by the increase in the proportion of forest landcover with decreasing altitude, as a proxy for increased distance from glacierized water sources and potentially more opportunity in wider, braided channels downstream to have warming influences of solar radiation.

The combined result of the upper White River basin SSN model predicting warmer water temperatures for the tributaries draining into the main stem and cooler water temperature for the upper White River main stem compared to the NorWeST model is attributed to upper White basin SSN model being calibrated with temperature data specific to the river. The NorWeST

SSN model had observations from lower elevation river reaches downstream and outside of the model of the model domain. This finding of different modeling results underscores the utility of local-scale models calibrated using local field observations from both glacierized and unglacierized basins if the scope of interest is similarly local.

Conclusions

Spatial stream network models predicted the spatial distribution of late-summer water temperature characterized by mean August and September water temperature and the seven-day average daily maximum of water temperature within the upper White River basin upstream of the White River's confluence with Silver Creek. Although each of these temperature metrics was correlated, the predictive performance of the AugTw and SepTw models was greatest, which was further improved by the inclusion of spatial autocovariance structures. The distribution of runoff from glacial meltwater throughout the White River basin network is likely a primary control on water temperature in both Aug and Sept as the proportion of basin ice landcover emerged as a significant covariate in the AugTw and SepTw models. The inclusion of this covariate in the models suggests that variability in water temperature can be explained by whether the drainage network includes or excludes runoff from glacial meltwater. The upper White River basin SSN model predicted warmer water temperatures for tributaries and cooler water temperatures for the main stem relative to the NorWeST SSN model. Differences in model estimates is attributed to the use of water temperature observations specifically from the upper White River study area, which were not included in the NorWeST model.

Acknowledgments

This study was funded by the National Park Service. This manuscript was improved by two USGS peer reviewers.

References Cited

Anderson, S.W. and Jaeger, K.L., 2020. Coarse sediment dynamics in a large glaciated river system: Holocene history and storage dynamics dictate contemporary climate sensitivity, GSA Bulletin, 133(5-6), 899-922. Accessed on July 10, 2024 at doi.org/10.1130/B35530.1.

Detenbeck, N.E., Morrison, A.C. Abele, R.W., and Kopp, D.A., 2016. Spatial statistical network models for stream and river temperature in New England, USA, Water Resources Research, 52,6018–6040, Accessed on July 10, 2024 at doi:10.1002/2015WR018349

Eby, L.A., Helmy, O., Holsinger, L.M., Young, M.K., 2014. Evidence of Climate-Induced Range Contractions in Bull Trout Salvelinus confluentus in a Rocky Mountain Watershed, U.S.A.. PLoS ONE 9(6): e98812. Accessed on July 10, 2024 at doi:10.1371/journal.pone.0098812

Gendaszek, A.S., Dunham, J.B., Torgersen, C.E., Hockman-Wert, D.P., Heck, M.P., Thorson, J., Mintz, J. and Allai, T., 2020. Land-cover and climatic controls on water temperature, flow permanence, and fragmentation of Great Basin stream networks. Water, 12(7), p.1962. Accessed on July 10, 2024 at https://www.mdpi.com/2073-4441/12/7/1962.

Haas, G. R. and J. D. McPhail, 2001. The post-Wisconsinan glacial biogeography of bull trout (Salvelinus confluentus): a multivariate morphometric approach for conservation biology and management, Canadian Journal of Fisheries and Aquatic Sciences, 58, Pages 2189– 2203.

Homer, C., Dewitz, J., Yang, L., Jin, S., Danielson, P., Xian, G., Coulston, J., Herold, N., Wickham, J., & Megown, K., 2015. Completion of the 2011 national land cover database for

the conterminous United States–representing a decade of land cover change information. Photogrammetric Engineering & Remote Sensing, 81(5), 345–354.

Isaak, D. J., C. H. Luce, B. E. Rieman, D. E. Nagel, E. E. Peterson, D. L. Horan, S. Parkes, and G. L. Chandler. 2010. Effects of climate change and wildfire on stream temperatures and salmonid thermal habitat in a mountain river network. Ecological Applications 20:1350–1371

Isaak, D.J., Wenger, S.J., Peterson, E.E., Ver Hoef, J.M., Nagel, D.E., Luce, C.H., Hostetler, S.W., Dunham, J.B., Roper, B.B., Wollrab, S.P., et al., 2017. The NorWeST summer stream temperature model and scenarios for the western US: A crowd-sourced database and new geospatial tools foster a user community and predict broad climate warming of rivers and streams. Water Resources Research, 53, 9181–9205.

Isaak, D.J., Luce, C.H., Horan, D.L., Chandler, G L., Wollrab, S.P., Dubois, W.B., and Nagel, D.E., 2020. Thermal regimes of perennial rivers and streams in the western United States. Journal of the American Water Resources Association, 56, 842–867. Accessed on July 10, 2024 at https://doi.org/10.1111/1752-1688.12864

Jaeger, K.L., Sando, R., Dunn, S.B., Gendaszek, A.S., 2023a. Predicting probabilities of late summer surface flow presence in a glaciated mountainous headwater region. Hydrological Processes, 37(2), e14813. Accessed on July 10, 2024 at https://doi.org/10.1002/hyp.14813.

Jaeger, K.L., Dunn, S.B., Wilkerson, O.A., 2023b. Supporting data for and predictions from streamflow permanence modeling in Mount Rainier National Park and surrounding area, Washington, 2018-2020: U.S. Geological Survey data release. Accessed on July 10, 2024 at https://doi.org/10.5066/P942QL23

Leach, A.C., Gendaszek, A.S., Jaeger, K.L., 2024, Stream Temperature Models of White River Watershed, Mount Rainier National Park, Washington: U.S. Geological Survey Data Release, https://doi.org/10.5066/P9ZKB3EZ.

McMahon T.E., Zale A.V., Barrows F.T., et al., 2007. Temperature and competition between bull trout and brook trout: a test of the elevation refuge hypothesis. Trans Amer Fish Soc 136: 1313–26.

National Park Service, 2024. Integrated Resource Management Applications (IRMA), Accessed on July 10, 2024 at https://irma.nps.gov/aqwebportal/.

Peterson, E.E., Hoef, J.M.V., 2914. STARS: An ArcGIS toolset used to calculate the spatial information needed to fit spatial statistical models to stream network data. J. Stat. Softw. 56, 1–17.

PRISM, 2021. Climate Group. Oregon State University Accessed on July 10, 2024 at https://prism.oregonstate.edu, data created 2021.

Rawhouser, A.K., Grace, L.P., Lofgren, R.A., Glesne, R.S., Boetsch, J.R, Welch, C.A., Samora, B.A., Crain, P., and Holmes, R.E., 2012. North Coast and Cascades Network water quality monit.oring protocol. Natural Resource Report NPS/NCCN/NRR—2012/571. National Park Service, Fort Collins, Colorado. Accessed on Jul 16, 2024 at https://irma.nps.gov/DataStore/DownloadFile/454917

Selong J.H., McMahon T.E., Zale A.V., Barrows F.T., 2001. Effect of temperature on growth and survival of bull trout, with application of an improved method for determining thermal tolerance in fishes. Trans Am Fish Soc130:1026–1037.

Steel, E.A., Sowder, C., Peterson, E.E., 2016. Spatial and temporal variation of water temperature regimes on the Snoqualmie River network. Journal of the American Water

Resources Association. 52(3): 769–787. Accessed on July 10, 2024 at doi:10.1111/1752-1688.12423.

Verhille, C.E., English, K.K., Cocherell, D.E., Farrell, A.P. and Fangue, N.A., 2016. High thermal tolerance of a rainbow trout population near its southern range limit suggests local thermal adjustment. Conservation Physiology, 4(1), p.cow057.

Ver Hoef, J.M., Peterson, E.E., 2010. A moving average approach for spatial statistical models of stream networks. J. Am. Stat. Assoc. 105, 6–18.